Acta Oncologica Vol. 32, No. 4, pp. 417–424, 1993

QUANTIFICATION OF APOPTOSIS AND NECROSIS BY FLOW CYTOMETRY

MICHAEL G. ORMEROD, XIAO-MING SUN, DAVID BROWN, ROGER T. SNOWDEN and GERALD M. COHEN

Apoptosis and necrosis are two important mechanisms of cell death. Several methods have recently been described for quantifying apoptotic cells by flow cytometry. We report a novel method for the quantification and separation of viable normal and apoptotic cells. We have applied this method both to immature rat thymocytes treated with a variety of agents and to a murine haemopoetic cell line after withdrawal of a growth factor. The cells were incubated with two dyes which give fluorescent complexes when bound to DNA, the bis-benzimidazole, Hoechst 33342, and propidium iodide. Three populations were identified and characterized. On excitation with UV radiation, dead cells fluoresced red due to the uptake of propidium iodide whereas apoptotic cells fluoresced bright blue; normal cells showed low blue, low red fluorescence. In this paper, we demonstrate how this method may be used to help to distinguish between cell death by apoptosis and necrosis.

Introduction

Two distinct modes of cell death—apoptosis and necrosis—have been recognized in eukaryotic cells (1–3). Apoptosis is involved in many normal biological processes, such as embryonic and T-cell development, metamorphosis and hormone-dependent atrophy (see reviews in (2) and (4)). It can also be induced by a variety of chemicals, including glucocorticoids (5) and chemotherapeutic agents which damage DNA (6). Apoptosis, which can be regarded as a mechanism of cell suicide, is characterized morphologically by condensation of nuclear chromatin, compaction of cytoplasmic organelles, cell shrinkage and changes at the cell surface (2, 3). Apoptotic cells in vivo are rapidly phagocytosed whereas in vitro rupture of the plasma membrane occurs only at a late stage. Biochemically, the most striking characteristic of apoptotic cells is the fragmentation of DNA into oligonucleosomal fragments with lengths which are multiples of 180–200 bp (3, 7, 8). In contrast, the hallmark of necrosis is uncontrolled swelling followed by rupture of the plasma membrane. The nucleus also swells but its major constituents are often recognizable at a late stage in the process (2). DNA degradation tends to be non-specific.

Conventional light and electron microscopy offer the best methods for detecting dying and dead cells and distinguishing between apoptosis and necrosis (1, 2). However, these techniques do not lend themselves to quantification. Biochemical measurements, such as estimation of DNA fragmentation (7), estimate the average property over a whole population. Flow cytometry has the advantage that measurements are made on large numbers of single cells with the bonus that selected populations can undergo fluorescence activated cell sorting.

Several papers have recently described flow cytometric methods for detecting apoptotic cells in lymphocytes and in cell lines derived from T and B cells or their tumours (9–24). Most of these methods necessitate fixing or permeabilizing the cells and only a few of them can simultaneously measure both necrotic and apoptotic cells. We have recently published a method, based on the uptake of the bis-benzimidazole dye, Hoechst 33342, which uses unfixed cells so that the apoptotic population can be sorted for further morphological and biochemical study. Hoechst 33342, which is taken up by viable cells, binds to AT rich regions in the minor groove of the DNA where it fluoresces blue under UV radiation. The method relies on the chance observation that some types of apoptotic cells

Received 23 November 1992.
Accepted 4 February 1993.
From MRC Toxicology Unit, Carshalton, Surrey, England (all authors).
Correspondence to: Dr M. G. Ormerod, 34 Wray Park Road, Reigate, Surrey RH2 ODE, England.
Presented at the symposium 'Analytical Cellular Pathology' in Umeå, October 5–6, 1992.

take up Hoechst 33342 more rapidly than normal cells (19, 22, 23). Cells with damaged plasma membranes, including necrotic cells, can be distinguished by adding propidium iodide (PI) which is excluded by viable cells and which fluoresces red on binding to the DNA of damaged cells.

In this article, we use the phrase 'dead' to describe cells which have damaged plasma membranes and are unable to exclude dyes such as trypan blue or PI. The term 'viable' is used to describe all cells with an intact plasma membrane including cells undergoing apoptosis.

Material and Methods

Material. Dexamethasone, etoposide, Hoechst 33342, and propidium iodide were obtained from Sigma Chemical Co. (Poole, England), zinc acetate dihydrate from Fisons Scientific (Loughborough, England), camptothecin, 4'-(9-acridinylamino) methanesulfon-m-anisidine (m-AMSA) and 4'-(9-acridinylamino) methanesulfon-o-anisidine (o-AMSA) from the Chemistry Branch, National Cancer Institute, Bethesda, Md., USA, fetal bovine serum (FBS) and RPMI-1640 from Gibco (Paisley, Scotland), Dulbecco's 'A' phosphate-buffered saline (PBS) from Unipath (Hampshire, England) and minimum essential medium from Flow Laboratories (Irvine, Scotland).

Cell culture. Murine IL-3-dependent BAF-3 cells (25) were cultured in RPMI medium containing 10% FBS, 1 mM glutamine and 5% conditioned medium from the IL-3 producing cell line, Wehi-3B. To induce apoptosis, the cells were washed twice and then cultured in the above medium without the addition of the conditioned medium.

Thymocytes. Male Fischer 344 rats, 4–5 weeks old, were bred at the MRC Toxicology Unit (Carshalton, England); murine thymocyte were obtained from CBA mice. Animals were given food and water ad libitum. Thymocytes were isolated as described previously (23). The cells were suspended in RPMI-1640 plus 10% FBS at a final concentration of about 2×10^7 ml^{-1}. Cells were incubated for 4–6 h at 37°C under an atmosphere of 95% air:5% CO_2, alone or with different drugs as described in the text.

Flow cytometry. Cells were analysed on an Ortho Cytofluorograf 50H linked to a 2150 computer system equipped with a Coherent argon-ion laser producing 200 mW at 488 nm and a Coherent krypton laser producing 50 mW at 352 nm. Univariate histograms and bivariate cytograms were transferred to an IBM-compatible PC for further analysis and preparation of figures using software

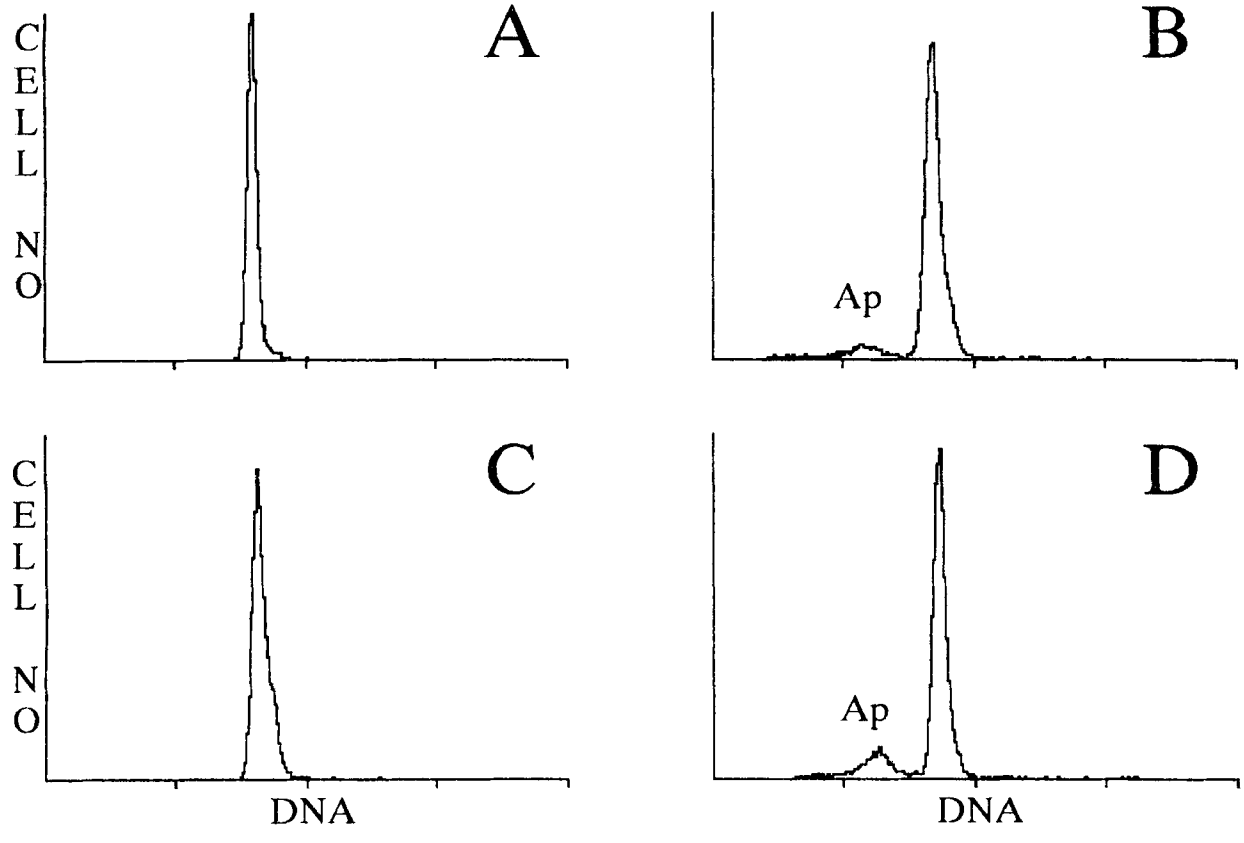

Fig. 1. DNA histogram from murine thymocytes incubated at 37°C after 3 Gy γ-radiation. The cells were fixed and incubated with PI and RNAase before recording red fluorescence excited by blue light. A sub-G1 peak, labelled 'Ap', appears with time of incubation. A) No radiation, 0 h; B) No radiation, 4 h; C) 3 Gy radiation, 0 h; D) 3 Gy radiation, 4h.

written by one of the authors (MGO). In order to record DNA histograms, about 10^6 cells were pelleted, resuspended in 200 μl PBS and fixed rapidly in 2 ml 70% ice-cold ethanol. Cells were centrifuged from the fixative, resuspended in 1 ml PBS, 10 μg/ml PI, 100 μg/ml RNAase and incubated at 37°C for 30 min. The excitation wavelength in the cytometer was 488 nm and red (> 630 nm) fluorescence was recorded. Pulse shape analysis was performed to eliminate any cell clumps (26). To discriminate between live, 'dead' and apoptotic cells, cells were incubated at 37°C in RPMI-1640 medium plus 10% FBS in the presence of 1 μg/ml Hoechst 33342 for 7 min for BAF-3 cells and 10 min for rat thymocytes. The cells were cooled on ice, centrifuged and the pellet resuspended in PBS, 5 μg/ml PI and kept on ice. The flow cytometer was used with the UV laser and forward light scatter, blue (400–500 nm) and red (> 630 nm) fluorescence recorded.

DNA gel electrophoresis and DNA fragmentation. Agarose gel electrophoresis was carried out as previously described (22). DNA fragmentation was measured by the percentage of diphenylamine reactive material present in the supernatant fraction obtained after centrifuging lysed cells at 13 000 G (27).

Results and Discussion

DNA histogram

Fig. 1 shows a DNA histogram recorded from some murine thymocytes after γ irradiation in vitro, a treatment which is known to cause cell death through apoptosis (28). The cells were fixed in ethanol and stained with PI. Before the cells were incubated at 37°C (time 0), the DNA histogram consisted predominantly of a single peak from cells in G1/G0 of the cell cycle. At later times, a hypodiploid ('sub-G1') peak, which increased with time of incubation in both irradiated and unirradiated cells, was evident, being greater after irradiation. A similar peak has

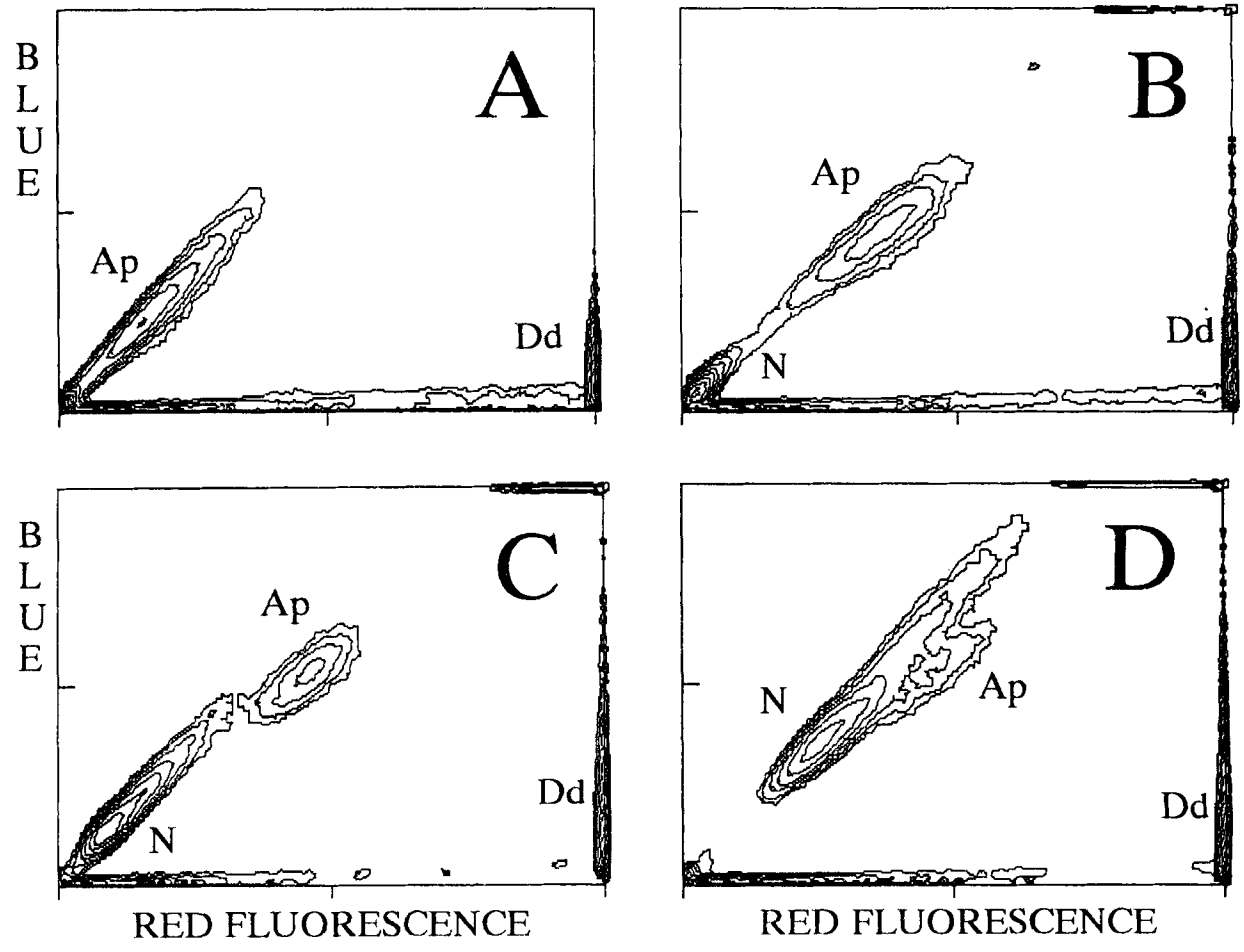

Fig. 2. Uptake of Hoechst 33342 by BAF-3 cells undergoing apoptosis; cytograms of blue (Hoechst-DNA) versus red fluorescence (PI-DNA). Cells, incubated in medium without IL3 for 16 h, were incubated with Hoechst 33342 (1 μg/ml) for the times shown, centrifuged and PI (5 μg/ml) added. The red PMT voltage was set in order to visualize the red fluorescence from Hoechst-DNA; the PI-DNA fluorescence from the 'dead' cells was consequently off-scale. N = normal cells; Ap = apoptotic cells; Dd = 'dead' cells. The times of incubation with Hoechst 33342 were: A) 5 min; B) 10 min; C) 20 min; D) 40 min.

been observed on the induction of apoptosis in various cellular systems, such as rat and murine thymocytes, a murine haemopoetic cell line and in human leukemic cell lines after γ irradiation, withdrawal of growth factor and treatment with glucocorticoids and topoisomerase I and II inhibitors (9–12, 14–18, 20, 22, 24). Darzynkiewicz et al. (20) have reviewed the current evidence and concluded that the reduced stainability of DNA in apoptotic cells represents a decrease in the DNA content and is not due to a change in the dye-DNA interaction.

Necrotic cells cannot be recognized in a conventional DNA histogram although in some systems it may be possible to distinguish them by light scatter (for example, see (18)). There is an alternative method of cell cycle measurement which distinguishes between dead and live cells. Unfixed cells are incubated with PI which stains the

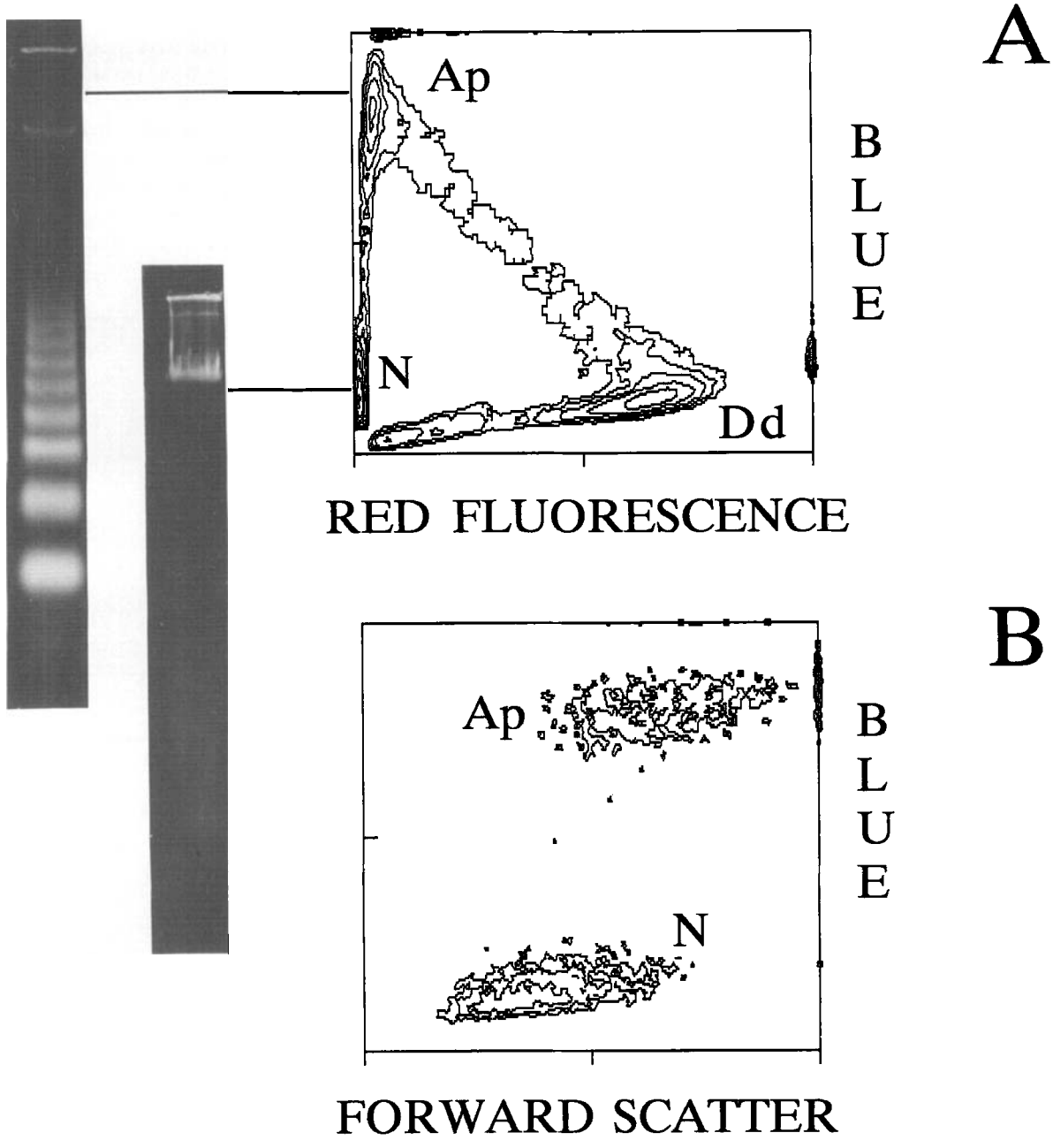

Fig. 3. BAF-3 cells undergoing apoptosis incubated for 7 min with Hoechst 33342, other details as in Fig. 2. A) Cytogram of blue (Hoechst-DNA) versus red fluorescence (PI-DNA). Alongside the cytogram are tracks from DNA gel electrophoresis of cells sorted from the clusters marked 'Ap' and 'N'. The apoptotic cells (Ap) gave characteristic DNA 'ladders' while the DNA in the normal (N) cells was of high molecular weight. B) Cytogram of blue (Hoechst-DNA) fluorescence versus forward light scatter after gating out the PI-positive (dead) cells on cytogram A.

DNA of dead cells; the cells are then fixed and stained with Hoechst 33342. On excitation with UV radiation, the dead cells fluoresce red from PI and the cell cycle of the live cells is revealed by the blue Hoechst fluorescence (29). In this method, the Hoechst-DNA histogram of the apoptotic cells showed a sub-G1 peak allowing identification of live, 'dead', and apoptotic cells (20).

For these assays, the cells must be fixed or permeabilized and these procedures limit the value of sorted cells for further biochemical or morphological study.

The Hoechst-PI method (19, 22, 23)

Murine haemopoetic cell line. The murine haemopoetic cell line, BAF3, requires interleukin-3 (IL3) for growth (25). If IL3 is removed, after 9 h, the cells start to undergo apoptosis (11, 22). These cells, 18 h after withdrawal of growth factor, were incubated with a low concentration of Hoechst 33342 (1 μg/ml), washed, PI added and a cytogram of blue (Hoechst-DNA) versus red (PI-DNA) fluorescence recorded. Fig. 2 shows the time course of uptake of Hoechst 33342. A separate cluster of cells could be identified which took up the Hoechst dye more rapidly and fluoresced more brightly. After extended incubation, this separate population could only be distinguished by a difference in the ratio of blue to red Hoechst-DNA fluorescence (Fig. 2). Cells from the rapidly staining population have been sorted and identified as apoptotic by light and electron microscopy and DNA gel electrophoresis (22). An example of the latter is shown in Fig. 3A; DNA extracted from cells sorted from the high blue, low red cluster ('Ap' in the Figure) gave a characteristic 'ladder' of nucleosomal fragments or multiples thereof. In contrast, DNA from cells sorted from the low blue, low red cluster ('N') was of high molecular weight. In the cytogram, cells 'tracking' between the apoptotic (high blue, low red fluorescence) and the 'dead' populations (low blue, high red) could be observed as well as dead cells whose DNA was being further degraded. In this system, the forward light scatter of the apoptotic cells was greater than that of the normal cells but this difference was insufficient on its own to distinguish between the two populations (Fig. 3B). The

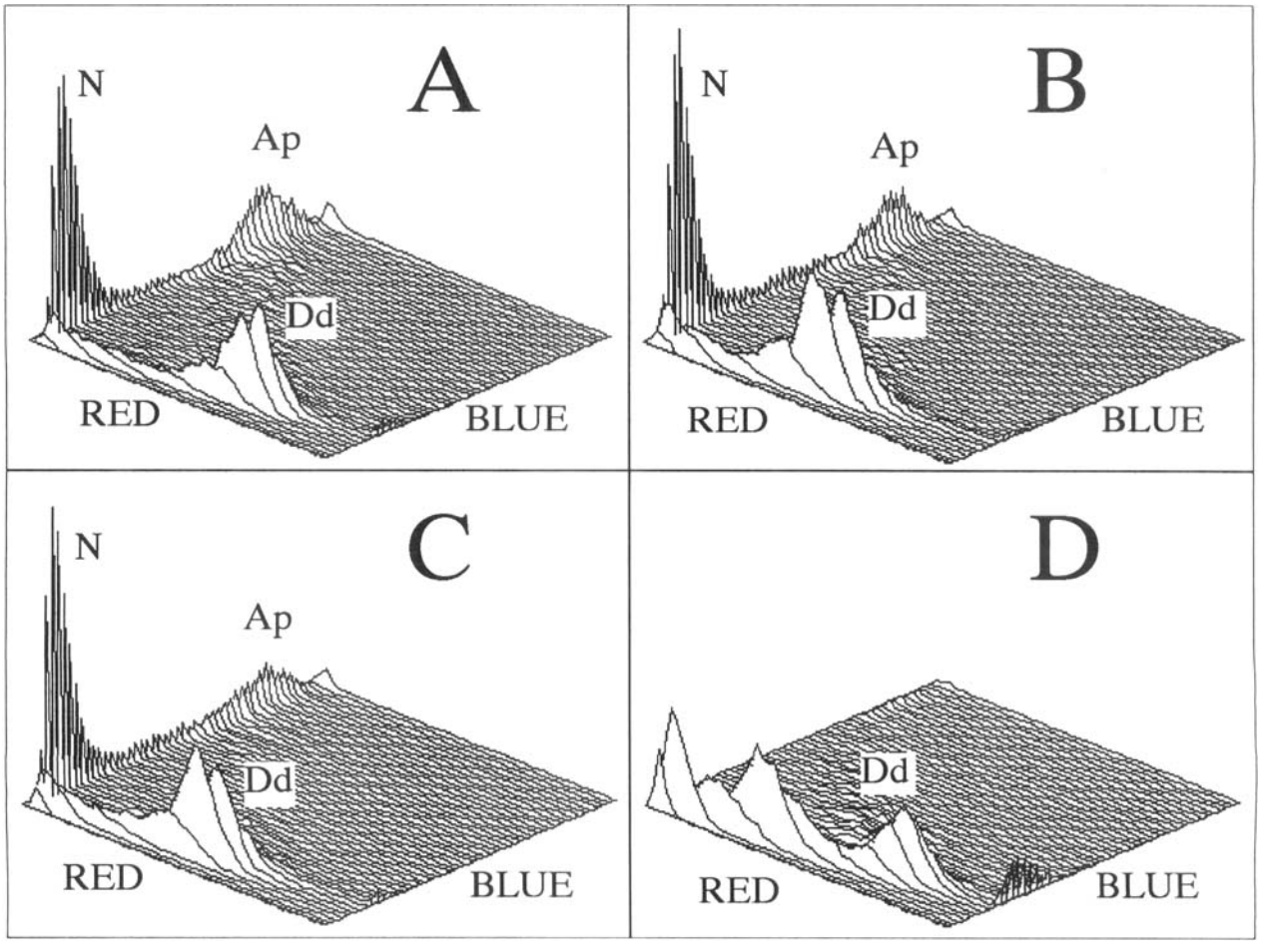

Fig. 4. The effect of Zn^{2+} on BAF-3 cells undergoing apoptosis. BAF3 cells were incubated for 16 h in the absence of IL3 and in the presence of different concentrations of zinc acetate. Cells were then incubated with Hoechst 33342 and PI added as in Figs 2 and 3. Labels as in Fig. 3. A) No Zn^{2+}; B) 20 μM Zn^{2+}; C) 100 μM Zn^{2+}; D) 500 μM Zn^{2+}.

ability to distinguish between apoptotic and necrotic cells was demonstrated when we investigated the effect of zinc acetate on this system (Fig. 4). Zn^{2+} inhibits the Ca^{2+}, Mg^{2+} dependent endonuclease which degrades the DNA in apoptotic cells into oligonucleosomal fragments (30). On the basis of the inhibition of DNA 'laddering', it has been reported that Zn^{2+} prevents apoptosis but we have shown that, in the presence of this ion, immature rat thymocytes treated with dexamethasone still undergo key morphological changes associated with apoptosis in the absence of DNA fragmentation (27). In contrast to thymocytes, over the period of 18 h used to induce apoptosis, BAF3 cells were susceptible to the cytotoxic effects of Zn^{2+}. At concentrations of zinc acetate greater than 100 μM, dead cells were observed while at 100 μM or less the production of apoptotic cells (as measured by high blue fluorescence) was not inhibited (Fig. 4).

Immature rat thymocytes. When the Hoechst-PI method was applied to immature rat thymocytes, it was found that an optimal separation between normal and apoptotic cells was obtained when a slightly longer time of incubation with Hoechst 33342 was used (10 min) (23). During apoptosis rat thymocytes shrink and become denser (3); this alteration was reflected in a dramatic decrease in the forward light scatter, thereby giving a second parameter with which to distinguish the normal and apoptotic populations (Fig. 5). This should be contrasted with the BAF3 cells in which the apoptotic cells scattered more light, emphasizing the importance of fully characterizing apoptotic cells for each cell type studied. We have sorted cells from the populations labelled apoptotic and normal and confirmed their classification using DNA gel electrophoresis and electron microscopy (23). Lyons et al. (21) have observed a small increase in the uptake of ethidium bromide in apoptotic murine thymocytes. The increase in the rates of uptake of both Hoechst 33342 and ethidium bromide may be caused by the same change in the plasma membrane of apoptotic thymocytes. We have used the Hoechst 33342/PI method to quantify the amount of apoptosis in thymocytes after treatment with a variety of

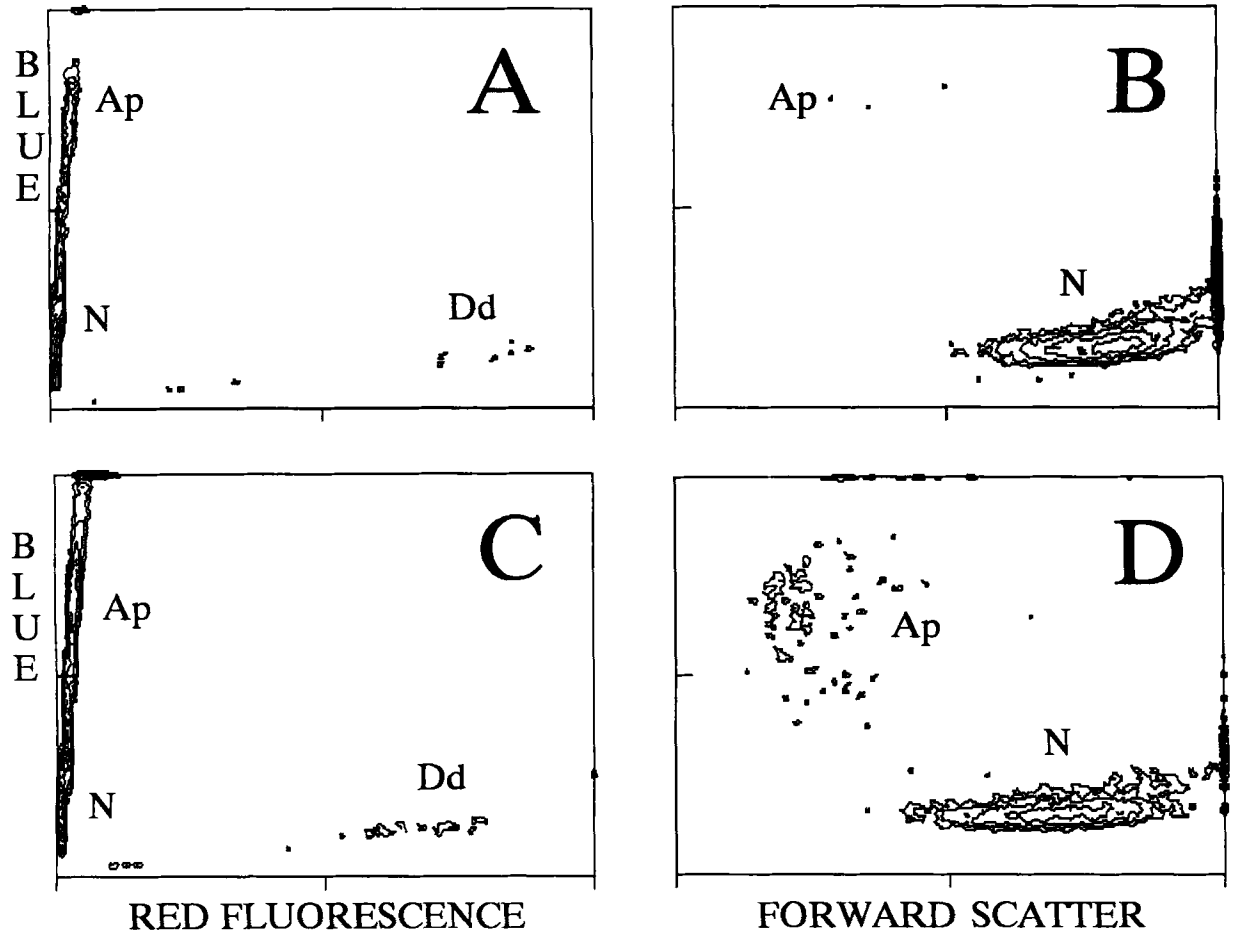

Fig. 5. Quantification of apoptotic rat thymocytes. Immature rat thymocytes were incubated alone (A, B) or with 0.1 μM dexamethasone (C, D) for 4 h and then with Hoechst 33342 (1 μg/ml) for 10 min. PI (5μg/ml) was added before analysis. A, C) Cytograms of blue (Hoechst/DNA) versus red (PI/DNA) fluorescence. B, D) Cytograms of blue fluorescence versus forward light scatter after gating out the PI positive cells on cytogram A or C. N = normal cells; Ap = apoptotic cells; Dd = 'dead' cells.

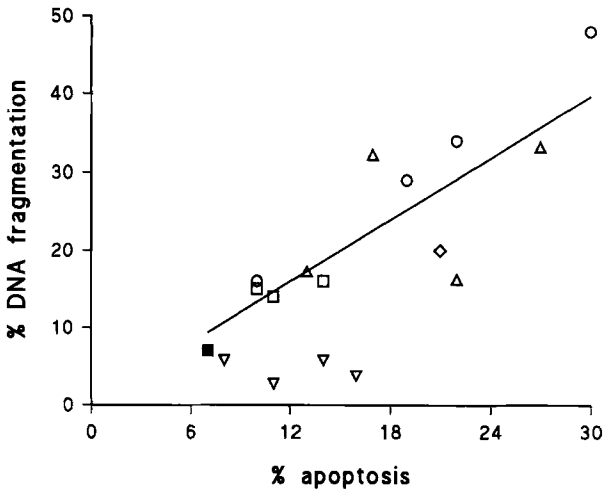

Fig. 6. Correlation between DNA fragmentation and percentage apoptotic cells in immature rat thymocytes after incubation for 4 h with different drugs. DNA fragmentation was the percent DNA in the supernatant fraction after centrifugation of lysed cells at 13 000 G; percentage apoptotic cells was measured by flow cytometry. ■—no drug; ◇—dexamethasone (0.1 μM); ○—etoposide (1, 5, 10, 25 μM); □—camptothecin (1, 10, 100 μM); △—m-AMSA (1, 5, 10, 25 μM); ▽—o-AMSA (1, 5, 10, 25 μM). The lie shown was fitted by linear regression analysis excluding the data from o-ASMA.

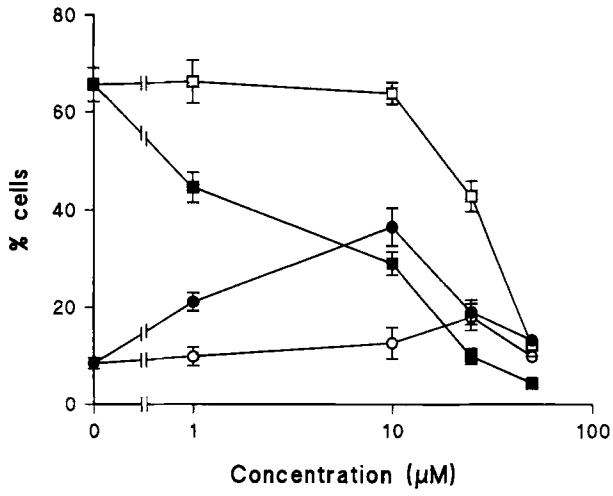

Fig. 7. Effect of m-AMSA and o-AMSA on immature rat thymocytes. Cells were incubated for 4 h with drug and the percentage of normal and apoptotic cells estimated by flow cytometry. Solid symbols—m-AMSA; open symbols—o-AMSA; □, ■—viability; ○, ● apoptosis.

compounds and have compared this to the amount of fragmented DNA measured by the diphenylamine method. The compounds used were the glucocorticoid, dexamethasone, the topoisomerase I inhibitor, camptothecin, the topoisomerase II inhibitors, eptoposide and m-AMSA and the structural isomer, o-AMSA. With the exception of the data obtained after treatment with o-AMSA, there was a good correlation between the two measurements further establishing the validity of the flow cytometric technique (Fig. 6). The apoptosis observed in the presence of o-AMSA was slightly increased above that from the untreated control cells while the amount of DNA fragmentation was the same or less than the control. Characteristic DNA 'ladders' were also absent from the DNA gels (data not shown). The presence of high blue cells in the flow cytometric assay without concomitant DNA fragmentation suggests that o-AMSA inhibits the specific endonuclease involved in the apoptotic process. We have previously shown that critical changes in apoptosis in thymocytes precede endonuclease activation (Cohen, Sun, Snowden, Ormerod and Dinsdale, submitted for publication) and that treatment of immature rat thymocytes with dexamethasone in the presence of zinc acetate induces apoptosis without DNA fragmentation (27). This previously unreported effect of o-AMSA clearly requires further study. The two isomers of AMSA also provide an example of the distinction of different mechanisms of cytotoxicity (Fig. 7). Immature rat thymocytes were treated with different concentrations of the isomers, m-AMSA and o-AMSA. At low concentrations, m-AMSA caused an increase in apoptosis above that seen in untreated cells while at increased concentrations, there was a large increase in 'dead' cells. At the lower concentrations, o-AMSA had a much smaller effect whereas at higher concentrations, the predominant effect was loss of viability. The flow cytometric data revealed two mechanisms of cell killing; at high doses of drug, necrosis was induced equally effectively by both isomers while at lower doses m-AMSA triggered apoptosis.

Concluding Discussion

It would be highly desirable to have a universal flow cytometric method for detecting apoptotic cells. Unfortunately, at present, the most reliable method of identifying apoptotic cells is morphological assessment. Flow cytometric methods which involve the observation of a hypodiploid or 'sub-G1' peak in the DNA histogram rely on extensive DNA degradation as part of the apoptotic process. However, it is not known whether endonuclease activation, which is undoubtedly important in many types of cell, is universal and we have also shown that this is a late event in apoptosis and can be divorced from key morphological changes ((27), and Cohen, Sun, Snowden, Ormerod and Dinsdale, submitted for publication).

It has been reported that there are alterations in the plasma membranes for apoptotic thymocytes (31, 32). The increased staining of thymocytes by Hoechst 33342 is due to an increased rate of uptake of the dye (Ormerod, Sun, Snowden, Davies, Fearnhead and Cohen, submitted for publication) presumably caused by a change in the properties of the plasma membrane. Although we have observed this effect in two systems, there is no reason to assume that such a change is a universal hallmark of apoptosis. Even,

in those types of cell in which this effect is observed, the method should still be used with caution since some drugs may induce changes in the properties of the plasma membrane independent of apoptosis. Despite its limitations, the Hoechst/PI method has advantages over other methods in the literature. It has enabled us to quantify and separate apoptotic rat thymocytes and, more recently, we have utilized the method to characterize a preapoptotic subpopulation of cells (Cohen, Sun, Snowden, Ormerod and Dinsdale, submitted for publication).

Any flow cytometric method for quantifying apoptotic cells must be validated in the cell system under study. Cell sorting should ideally be combined with light and electron microscopy.

REFERENCES

1. Kerr JFR, Wyllie AH, Currie AR. Apoptosis: a basic biological phenomenon with wide ranging implications in tissue kinetics. Br J Cancer 1972; 26: 239–57.
2. Wyllie AH, Kerr JFR, Currie AR. Cell death: the significance of apoptosis. Int Rev Cytology 1980; 68: 251–305.
3. Arends MJ, Wyllie AH. Apoptosis: mechanisms and role in pathology. Int Rev Exp Pathol 1991; 32: 223–54.
4. Ellis RE, Yuan J, Horvitz HR. Mechanisms and function of cell death. Ann Rev Cell Biol 1991; 7: 663–98.
5. Cohen JJ. Programmed cell death in the immune system. Adv Immunol 1991; 50: 55–85.
6. Barry MA, Behnke CA, Eastman A. Activation of programmed cell death (apoptosis) by cisplatin, other anticancer drugs, toxins and hyperthermia. Biochem Pharmacol 1990; 40: 2353–62.
7. Wyllie AH. Glucocorticoid-induced thymocyte apoptosis is associated with endonuclease activation. Nature 1980; 284: 555–6.
8. Wyllie AH, Morris RG, Smith AL, Dunlop D. Chromatin cleavage in apoptosis: association with condensed chromatin morphology and dependence on macromolecular synthesis. J Pathology 1984; 142: 67–77.
9. Compton MM, Haskill JS, Cidlowski JA. Analysis of glucocorticoid actions on rat thymocyte deoxyribonucleic acid by fluorescence-activated flow cytometry. Endocrinol 1988; 122: 2158–64.
10. Ojeda F, Guarda MI, Maldonado C, Folch H. Protein kinase-C involvement in thymocyte apoptosis induced by hydrocortisone. Cell Immunol 1990; 125: 535–9.
11. Rodriguez-Tarduchy G, Collins M, Lopez-Rivas A. Regulation of apoptosis in interleukin-3-dependent hemopoietic cells by interleukin-3 and calcium ionophores. EMBO J 1990; 9: 2997–3002.
12. Nicoletti I, Migliorati G, Pagliacci MC, Griganani F, Riccardi C. A rapid and simple method for measuring thymocyte apoptosis by propidium iodide staining and flow cytometry. J Immunol Methods 1992; 139: 271–9.
13. Swat W, Ignatowicz L, Kisielow P. Detection of apoptosis of immature CD4 + 8 + thymocytes by flow cytometry. J Immunol Methods 1991; 137: 79–87.
14. Telford WG, King LE, Fraker PJ. Evaluation of glucocorticoid-induced DNA fragmentation in mouse thymocytes by flow cytometry. Cell Prolif 1991; 24: 447–9.
15. Telford WG, King LE, Fraker PJ. Comparative evaluation of several DNA binding dyes in the detection of apoptosis-associated chromatin degradation by flow cytometry. Cytometry 1991; 13: 137–43.
16. Bruno S, Lassota P, Giaretti W, Darzynkiewicz Z. Apoptosis of rat thymocytes triggered by prednisolone, camptothecin or teniposide is selective to G0 cell and is prevented by inhibitors of proteases. Oncol Res 1992; 4: 29–35.
17. Hotz MA, Traganos F, Darzynkiewicz Z. Changes in nulcear chromatin related to apoptosis or necrosis induced by the DNA topoisomerase II inhibitor fostriecin in Molt-4 and HL-60 cells are revealed by altered DNA sensitivity to denaturation. Expl Cell Res 1992; 201: 184–91.
18. Jones TL, Lafrenz D. Quantitative determination of the induction of apoptosis in a murine B cell line using flow cytometric bivariate cell cycle analysis. Cell Immunol 1992; 142: 348–60.
19. Dive C, Gregory CD, Phipps DJ, Evans DL, Milner AE, Wyllie AH. Analysis and discrimination of necrosis and apoptosis (programmed cell death) by multiparameter flow cytometry. Biochim Biophys Acta 1992; 1133: 275–85.
20. Darzynkiewicz Z, Bruno S, Del Bino G et al. Features of apoptotic cells measured by flow cytometry. Cytometry 1992; 13: 795–808.
21. Lyons AB, Samuel K, Sanderson A, Maddy AH. Simultaneous analysis of immunophenotyping and apoptosis of murine thymocytes by single laser flow cytometry. Cytometry 1992; 13: 809–21.
22. Ormerod MG, Collins MKL, Rodriguez-Tarduchy G, Robertson D. Apoptosis in interleukin-3-dependent haemopoetic cells. Quantification by two flow cytometric methods. J Immunol Methods 1992; 153: 57–65.
23. Sun X-M, Snowden RT, Skilleter DN, Dinsdale D, Ormerod MG, Cohen GM. A flow cytometric method for the separation and quantitation of normal and apoptotic thymocytes. Anal Biochem 1992; 204: 351–6.
24. Walker PR, Smith C, Youdale T, Lebland J, Whitfield JF, Sikorska M. Topoisomerase II-reactive chemotherapeutic drugs induce apoptosis in thymocytes. Cancer Res 1991; 51: 1078–85.
25. Palacios R, Steinmetz M. IL3-dependent mouse clones that express B-220 surface antigen, contain Ig genes in germ-line configuration and generate B lymphocytes in vivo. Cell 1985; 41: 727–30.
26. Ormerod MG. Analysis of DNA. General methods. In: Ormerod MG, ed. Flow cytometry. A practical approach. Oxford: IRL Press at Oxford University Press, 1990: 69–87.
27. Cohen GM, Sun X-M, Snowden RT, Dinsdale D, Skilleter DN. Key morphological features of apoptosis may occur in the absence of internucleosomal DNA fragmentation. Biochem J 1992; 286: 331–4.
28. Yamada T, Ohyama H. Radiation-induced interphase death of rat thymocytes is internally programmed (apoptosis). Int J Radiat Biol 1988; 53: 65–75.
29. Pollack A, Ciancio G. Cell-cycle phase specific analysis of cell viability using Hoechst 33342 and propidium iodide after ethanol preservation. In: Darzynkiewicz Z, Crissman HA, eds. Flow cytometry. San Diego, CA: Academic Press, 1991: 19–24.
30. Cohen JJ, Duke RC. Glucocorticoid activation of a calcium-dependent endonucleaase in thymocyte nuclei leads to cell death. J Immunol 1984; 132: 38–42.
31. Fadok VA, Voelker R, Cambell PA, Cohen JJ, Bratton DL, Henson PM. Exposure of phosphatidylserine on the surface of apoptotic lymphocytes triggers specific recognition and removal by macrophages. J Immunol 1992; 148: 2207–16.
32. Morris RG, Hargreaves AD, Duvall E, Wyllie AH. Hormone-induced cell death. 2. Surface changes in thymocytes undergoing apoptosis. Am J Pathol 1984; 115: 426–36.